Pergamon

Int. J. Solids Structures Vol. 33, No. 20-22, pp. 3081-3101, 1996

0020 7683/96 \$15.00 + .00

0020-7683(95)00272-3

EMBEDDED LOCALIZATION BAND IN UNDRAINED SOIL BASED ON REGULARIZED STRONG DISCONTINUITY—THEORY AND FE-ANALYSIS

R. LARSSON
Department of Structural Mechanics, Chalmers University of Technology, S-412 96 Göteborg, Sweden

K. RUNESSON
Division of Solid Mechanics, Chalmers University of Technology, S-412 96 Göteborg, Sweden

and

S. STURE
Department of Civil, Architectural and Environmental Engineering, University of Colorado, Boulder, CO 80309-0428, U.S.A.

Abstract—The paper presents a novel approach to the analysis of a developing localization zone in undrained soil considered as a mixture of a solid skeleton and fluid-filled pores, where the solid phase is considered as elastic–plastic. The basic feature is the concept of regularized displacement and pore pressure discontinuities, which are assumed to occur across an internal discontinuity surface. In this respect the present developments are extensions of those suggested by Simo *et al.* (1993), *Comput. Mech.* **12,** 277–296, and, more recently, by Larsson and Runesson (1995), *J. Engng Mech. ASCE* (in press). A finite element formulation is proposed on the basis of a mixed variational formulation in the spirit of the "enhanced strain" concept by Simo and Rifai (1990), *Int. J. Numer. Meth. Engng* **29,** 1595–1638. In this fashion, the localization zone is embedded into a "base" element for the ordinary analysis of the (non-localized) mixture problem. Copyright © 1996 Elsevier Science Ltd.

1. INTRODUCTION

Analyses of localized failure in porous materials, viz. soils, have predominantly been restricted to one-phase materials; thus aiming for the description of failure under drained conditions. In general, however, the pores are (at least partly) filled with a fluid, such as water, oil. etc., which means that the behavior of the soil mass is influenced by the drainage conditions for the pore fluid. In the general situation the deformation process becomes time-dependent due to the temporal variation of the excess pore pressure distribution, as induced by external loading (or environmental impact) and subsequently enhanced by shear band development. Shear band development may induce a (dramatic) increase of drainage capacity, as discussed by e.g. Desrue *et al.* (1993). However, there are also extreme situations when the soil mass (and the shear band) may be considered as undrained. This is of particular relevance for the analysis of fine-grained soils, such as silt and clay, which are saturated with pore fluid and possess a very low permeability. This is the only situation considered in the present paper.

A method is proposed for capturing the development of (effective) stress and excess pore pressure inside a shear band. The formulation is based on the introduction of suitably regularized discontinuous displacement and pore pressure fields, cf. Simo *et al.* (1993), Larsson *et al.* (1993) and Larsson and Runesson (1995), for one-phase continua. Similar analyses have previously been carried out for two-phase materials, e.g. Loret and Prevost (1990), but not within the framework of discontinuous displacement formulation. In this context, we note that Runesson *et al.* (1995) show that the localization characteristics are quite sensitive to the constraint imposed by the no-drainage assumption. For completely incompressible soil, which is pertinent to the special case of undrained behavior with an incompressible fluid, the surprising result was obtained that the critical band orientation is 45° to a principal stress axis for a very large class of elastic–plastic materials.

We pursue the analysis along the lines set out by Larsson and Runesson (1995), where the existence of a regularized displacement discontinuity is assessed from the condition of traction continuity across a narrow band, which may also be interpreted as preserved divergence of the stress across the band. These ideas are extended to include also a "matching" discontinuous pore pressure field. As a result, the ordinary localization problem will be generalized to include the continuity equation for the mixture of soil and pore fluid. A similar analysis has also been considered by Rudnicki (1983), although not within the present framework of regularized discontinuities.

It appears that it is convenient to establish the finite element approximation in such a way that nodal values represent the continuous (= compatible) portions of the displacement and pore pressure fields. As to the representation of the strain, we resort to the "enhanced strain approach", Simo and Rifai (1990). A mixed variational formulation is thereby introduced for the equilibrium equation and the mass balance equation (of fluid–solid). This means that the independent fields in the final FE-problem are the displacement and enhanced strain (cf. Larsson and Runesson (1995)), together with the pore pressure and enhanced pore pressure.

2. BALANCE AND CONSTITUTIVE RELATIONS FOR SOIL WITH PORE FLUID

Denoting by $\mathbf{s}$ the total stress in the mixture of solid and fluid, we may formulate the equilibrium equation simply as

$$-\nabla\cdot\mathbf{s} = \mathbf{b}, \tag{1}$$

where $\mathbf{b}$ is the bulk volume force. According to the "effective stress principle", the constitutive law for $\mathbf{s}$ is written as

$$\mathbf{s} = \boldsymbol{\sigma} - p\boldsymbol{\delta}, \quad \dot{\boldsymbol{\sigma}} = \mathbf{E}:\dot{\boldsymbol{\varepsilon}}, \tag{2}$$

where $\boldsymbol{\sigma}$ is the "effective stress", p is the excess pore fluid pressure and $\boldsymbol{\delta}$ is the second order identity tensor. For reasons that are given below, we shall henceforth denote $\boldsymbol{\sigma}$ the "solid stress" (instead of "effective stress", which is common in the soil mechanics literature).

As to the continuum tangent stiffness modulus tensor $\mathbf{E}$ introduced in eqn (2), we shall confine the analysis to small strain plasticity theory, in which case $\mathbf{E}$ is defined as

$$\mathbf{E} = \begin{cases} \mathbf{E}^{\mathrm{ep}} \equiv \mathbf{E}^{\mathrm{e}} - \dfrac{1}{h}\mathbf{E}^{\mathrm{e}}:\mathbf{gf}:\mathbf{E}^{\mathrm{e}} & \text{if } \mathbf{f}:\mathbf{E}^{\mathrm{e}}:\dot{\boldsymbol{\varepsilon}} > 0 \ (P) \\ \mathbf{E}^{\mathrm{e}} & \text{if } \mathbf{f}:\mathbf{E}^{\mathrm{e}}:\dot{\boldsymbol{\varepsilon}} \leqslant 0 \ (E) \end{cases}, \tag{3}$$

where (P) and (E) stand for "plastic" and "elastic" loading, respectively. In eqn (3), $\mathbf{E}^{\mathrm{e}}$ is the elastic stiffness modulus tensor, whereas $\mathbf{E}^{\mathrm{ep}}$ is the elastic–plastic tangent modulus tensor. Moreover, $\mathbf{f}$ is the gradient (in stress space) of the yield function, $\mathbf{g}$ is the flow direction ($\mathbf{g} \neq \mathbf{f}$ defines a non-associated flow rule). The scalar h is defined as

$$h = \mathbf{f}:\mathbf{E}^{\mathrm{e}}:\mathbf{g} + H > 0, \tag{4}$$

where H is a generalized hardening modulus. We distinguish between hardening ($H > 0$), perfect plasticity ($H = 0$) and softening ($H < 0$).

Remark. In a more general setting of the constitutive relations, we may introduce the scalar damage variable α as a measure of distributed failure in the solid skeleton ($0 \leqslant \alpha \leqslant 1$, where $\alpha = 0$ indicates the virgin state, whereas $\alpha = 1$ indicates complete deterioration). The

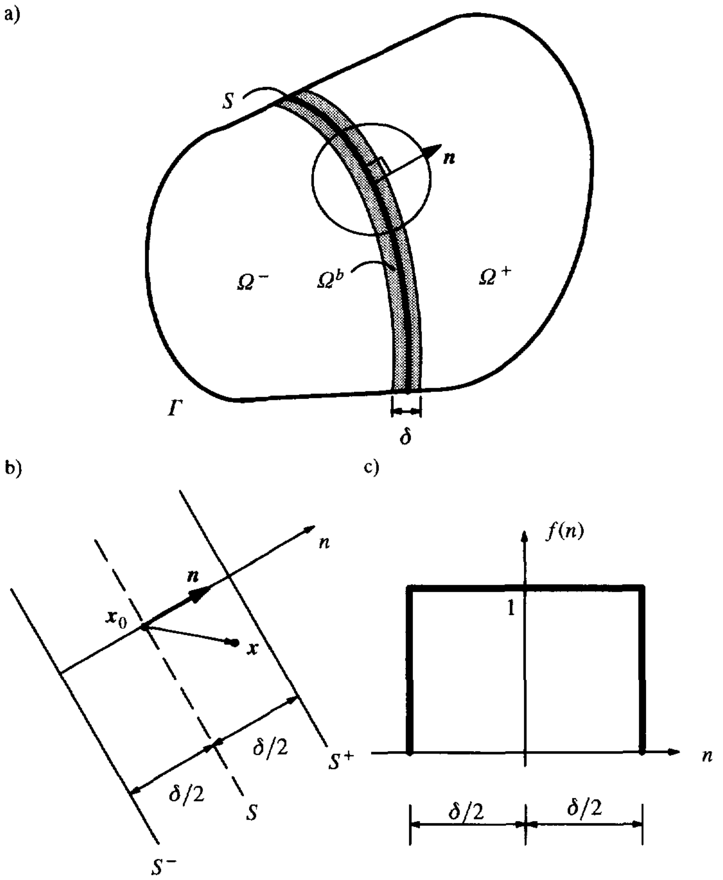

Fig. 1. (a) Solid with regularized discontinuity across internal surface S, (b) coordinates of localization band and (c) "irregular" block function.

relation between the "nominal stress" $\boldsymbol{\sigma}$ and the "effective stress" $\hat{\boldsymbol{\sigma}}$ is given as $\hat{\boldsymbol{\sigma}} = \boldsymbol{\sigma}/(1-\alpha)$. This is the motivation for introducing the notation "solid stress" for $\boldsymbol{\sigma}$. ●

Besides equilibrium, it is necessary to establish mass balance for the mixture of solid and fluid, which in the general situation takes the simple form

$$\nabla \cdot \boldsymbol{v} = -\dot{\varepsilon}_v + \dot{\varepsilon}_v^f \tag{5}$$

where $\boldsymbol{v}$ is the drainage flux of fluid (relative to the solid skeleton), $\dot{\varepsilon}_v = \dot{\boldsymbol{\varepsilon}} : \boldsymbol{\delta}$ is the rate of volumetric strain of the solid skeleton, and $\dot{\varepsilon}_v^f$ is the rate of volume change of the pore fluid (where positive $\dot{\varepsilon}_v$ means expansion). The following constitutive laws are adopted:

$$\boldsymbol{v} = -\mathbf{K} \cdot \nabla p, \quad \dot{\varepsilon}_v^f = -\frac{1}{K^f}\dot{p}, \tag{6}$$

where $\mathbf{K}$ is the Darcian (state-dependent) permeability tensor, whereas K^f is the compression modulus of the pore fluid. In the undrained situation we assume that $\nabla \cdot \boldsymbol{v} = 0$ (which is the result of rapid loading or vanishingly small permeability, i.e. $\mathbf{K} = \mathbf{0}$).

3. LOCALIZATION CONDITION

3.1. *Regularized discontinuous fields*

We shall pursue the analysis along the lines set out by Larsson and Runesson (1995) for the conventional one-phase (fully drained) material. It is then assumed that the soil occupies the domain Ω with external boundary Γ, as shown in Fig. 1(a). We consider the scenario where all state variables, including the displacement $\mathbf{u}(\mathbf{x})$ and the pore pressure $p(\mathbf{x})$, are continuous fields until the state is achieved, in the course of the deformation process, where localization is possible. At this state, it is assumed that a displacement discontinuity starts to develop along the internal surface S with the unit normal $\mathbf{n}$. The surface divides Ω into the sub-domains Ω^- and Ω^+ in such a way that $\mathbf{n}$ is pointing from Ω^- to Ω^+, as shown in Fig. 1(a). (It is emphasized that the onset of localization is merely a special case of this quite general kinematic format.)

We now propose the decomposition of the displacement field $\mathbf{u}(\mathbf{x}, t)$ as

$$\mathbf{u}(\mathbf{x}, t) = \mathbf{u}_c(\mathbf{x}, t) + [[\mathbf{u}(t)]]H_s(\mathbf{x}), \tag{7}$$

where $H_s(\mathbf{x})$ is the Heaviside function, centered on S, and $[[\mathbf{u}(t)]]$ is the *spatially constant* jump of $\mathbf{u}(\mathbf{x}, t)$ across S. Upon representing $\mathbf{x} \in \Omega$ as $\mathbf{x} = \mathbf{x}_0 + n\mathbf{n}(\mathbf{x}_0)$, where $\mathbf{x}_0 \in S$, we define the jump as

$$[[\mathbf{u}(t)]] = \lim_{\varepsilon \to 0}[\mathbf{u}(\mathbf{x}_0 + \varepsilon\mathbf{n}, t) - \mathbf{u}(\mathbf{x}_0 - \varepsilon\mathbf{n}, t)]. \tag{8}$$

The Heaviside function, introduced in eqn (7), is defined as

$$H_S(\mathbf{x}) = \begin{cases} 0 & \text{if } \mathbf{x} \in \Omega^- \\ 1 & \text{if } \mathbf{x} \in \Omega^+ \end{cases}. \tag{9}$$

As to the gradient of $H_S(\mathbf{x})$, we define the Dirac delta $\boldsymbol{\delta}_S(\mathbf{x})$ by the identity $\boldsymbol{\delta}_S(\mathbf{x}) = \nabla H_S(\mathbf{x})$ in the distributional sense

$$\int_\Omega \boldsymbol{\Psi} \cdot \boldsymbol{\delta}_s \, \mathrm{d}\Omega = \int_\Omega \boldsymbol{\Psi} \cdot \nabla H_s \, \mathrm{d}\Omega = \int_S \boldsymbol{\Psi} \cdot \mathbf{n} \, \mathrm{d}\Gamma \quad \forall \boldsymbol{\Psi} \in C_0^\infty(\Omega). \tag{10}$$

A regularized version of $\boldsymbol{\delta}_S(\mathbf{x})$ is obtained upon the introduction of a narrow band zone Ω^b (b = band) along S with the width δ, as shown in Fig. 1(a). The natural regularization of $\boldsymbol{\delta}_S(\mathbf{x})$, corresponding to a linear variation of $\mathbf{u}(\mathbf{x}, t)$ across Ω^b, is given as

$$\boldsymbol{\delta}_{s,r}(\mathbf{x}) = \frac{f(n)}{\delta}\mathbf{n}(\mathbf{x}_0), \quad n = \mathbf{n} \cdot (\mathbf{x} - \mathbf{x}_0), \tag{11}$$

where $f(n)$ is the irregular "block" function [shown in Fig. 1(c)] which is given as

$$f(n) = \begin{cases} 1 & \text{if } |n| < \dfrac{\delta}{2} \\[1ex] \dfrac{1}{2} & \text{if } |n| = \dfrac{\delta}{2} \\[1ex] 0 & \text{if } |n| > \dfrac{\delta}{2} \end{cases}. \tag{12}$$

(In order to simplify notation, we henceforth drop $\mathbf{x}$ and $\mathbf{x}_0$ as arguments when there is no risk of misunderstanding.) It then follows that eqn (11) represents a consistent regularization, i.e. $\boldsymbol{\delta}_{s,r}(\mathbf{x}) \to \delta_s(\mathbf{x})$ in the sense that

$$\int_{\Omega} \boldsymbol{\Psi} \cdot \boldsymbol{\delta}_{s,r} \, d\Omega = \frac{1}{\delta} \int_{\Omega^b} \boldsymbol{\Psi} \cdot \mathbf{n} \, d\Omega \rightarrow \int_S \boldsymbol{\Psi} \cdot \mathbf{n} \, d\Gamma \quad \text{when } \delta \rightarrow 0. \tag{13}$$

We interpret the narrow zone Ω^b (b = band) along S of width δ as the *localization zone*, as shown in Fig. 1(a). The remaining part of Ω is denoted $\Omega^{\pm} = \Omega^+ \cup \Omega^-$.

The strain $\boldsymbol{\varepsilon}(\mathbf{x}) = (\nabla\mathbf{u}+\mathbf{u}\nabla)/2$, and its corresponding volumetric portion $\varepsilon_v(\mathbf{x}) = \nabla \cdot \mathbf{u}$, can now be expressed in the regularized form as

$$\boldsymbol{\varepsilon} = \boldsymbol{\varepsilon}_c + \frac{f(n)}{2\delta}(\mathbf{n}[[\mathbf{u}]] + [[\mathbf{u}]]\mathbf{n}) \tag{14a}$$

$$\varepsilon_v = \varepsilon_{v,c} + \frac{f(n)}{\delta}\mathbf{n} \cdot [[\mathbf{u}]], \tag{14b}$$

where $\boldsymbol{\varepsilon}_c = (\nabla\mathbf{u}_c + \mathbf{u}_c\nabla)/2$ and $\dot{\varepsilon}_{v,c} = \nabla \cdot \mathbf{u}_c$ are the regular (continuous) parts.

Conservation of momentum and mass, as expressed in eqns (1) and (5), must always be preserved inside as well as outside the localization band. In fact, these are the conditions that will determine whether it is possible or not to initiate (and maintain) discontinuous displacement and pore-pressure fields.

Remark. We emphasize that the decomposition (7) must be interpreted in the sense that the displacement jump is spatially constant in the neighborhood of an arbitrary point $\mathbf{x}_0 \in S$. Hence, eqn (7) is of a local character, which, in the variational formulation of the boundary value problem, is never realized as the actual separation of the sub-domains Ω^- and Ω^+. At the numerical treatment (discussed subsequently), it is rather the strain pertinent to a regularized version of eqn (7) that is considered piecewise constant within each finite element, whereby the displacement discontinuity is constant within each element. However, the discontinuity may indeed differ from one element to another.●

3.2. *Momentum balance*

We start by considering the momentum balance in an incremental format (at a post-localized state). By invoking eqn (14a) into the constitutive relation (2b), we may express the (solid) stress rate $\dot{\boldsymbol{\sigma}}$ as

$$\dot{\boldsymbol{\sigma}} = \dot{\boldsymbol{\sigma}}_c + f(n)[[\mathbf{E}]] : \dot{\boldsymbol{\varepsilon}}_{c(b)} + \frac{f(n)}{\delta}(\mathbf{E}_{(b)} \cdot \mathbf{n}) \cdot [[\dot{\mathbf{u}}]], \tag{15}$$

where the subindex b refers to a value within the band. It is tacitly used that $\boldsymbol{\varepsilon}_c$ is continuous and that δ is a small measure, such that $\boldsymbol{\varepsilon}_{c(b)} = \boldsymbol{\varepsilon}_c(\mathbf{x}_0)$ represents the strain in the band. The regular part of $\dot{\boldsymbol{\sigma}}$ is $\dot{\boldsymbol{\sigma}}_c = \mathbf{E}_c : \dot{\boldsymbol{\varepsilon}}_c$. We have also introduced the notation $\mathbf{E}_{(b)} = \mathbf{E}(\mathbf{x}_0)$ and $\mathbf{E}_{c(b)} = \mathbf{E}_c(\mathbf{x}_0)$ for values of the tangent stiffness tensor within the band. These values are associated with an appropriate loading situation (plastic loading or elastic unloading) that is determined by $\dot{\boldsymbol{\varepsilon}}_{(b)}$ and $\dot{\boldsymbol{\varepsilon}}_{c(b)}$, respectively. Plastic loading inside and outside the band is thus defined as

$$\mathbf{f} : \mathbf{E}^e : \dot{\boldsymbol{\varepsilon}}_{(b)} = \mathbf{f} : \mathbf{E}^e : \dot{\boldsymbol{\varepsilon}}_{c(b)} + \frac{1}{\delta}\mathbf{a}[[\dot{\mathbf{u}}]] > 0, \quad \mathbf{f} : \mathbf{E}^e : \dot{\boldsymbol{\varepsilon}}_{c(b)} > 0 \quad \mathbf{x} \in \Omega^b \tag{16a}$$

$$\mathbf{f} : \mathbf{E}^e : \dot{\boldsymbol{\varepsilon}}_c > 0 \quad \mathbf{x} \in \Omega^{\pm}, \tag{16b}$$

where the vectors $\mathbf{a}(\mathbf{n})$ (and $\mathbf{b}(\mathbf{n})$ for later use) are defined as

$$\mathbf{a}(\mathbf{n}) = \mathbf{f} : \mathbf{E}^e \cdot \mathbf{n}, \quad \mathbf{b}(\mathbf{n}) = \mathbf{n} \cdot \mathbf{E}^e : \mathbf{g}. \tag{17}$$

Moreover, $[[\mathbf{E}]] = \mathbf{E}_{(b)} - \mathbf{E}_{c(b)}$ is the jump in tangent stiffness.

Remark. The expression for $\dot{\boldsymbol{\sigma}}$ in eqn (17) is valid inside as well as outside the band Ω^b. For example, $\mathbf{x} \in \Omega^{\pm}$ is defined by $|n| > \delta/2$ in which case $\dot{\boldsymbol{\sigma}} \equiv \dot{\boldsymbol{\sigma}}_c$. Inside the band the quantity $\dot{\boldsymbol{\sigma}}_c = \dot{\boldsymbol{\sigma}}_{c(b)}$ is well-defined, although it does not correspond to any physical deformation mode. ●

As to the excess pore pressure, we propose that it has the same regularity as $\boldsymbol{\sigma}$, i.e.

$$p = p_c + f(n)[[p]], \tag{18}$$

where $[[p]] = p_{(b)} - p_{c(b)}$ is the jump due to irregularity. We may combine eqn (18) with eqn (15) to obtain

$$\dot{\mathbf{s}} = \dot{\mathbf{s}}_c + f(n)[[\mathbf{E}]] : \dot{\boldsymbol{\varepsilon}}_{c(b)} + \frac{f(n)}{\delta}(\mathbf{E}_{(b)} \cdot \mathbf{n}) \cdot [[\dot{\mathbf{u}}]] - f(n)\boldsymbol{\delta}[[\dot{p}]] \tag{19}$$

with $\dot{\mathbf{s}}_c = \dot{\boldsymbol{\sigma}}_c - \dot{p}_c \boldsymbol{\delta}$.

From the requirement that momentum must be conserved inside as well as just outside the band, we now obtain the conditions

$$-\nabla \cdot \dot{\mathbf{s}} = \mathbf{b} \quad \text{for } \mathbf{x} = \mathbf{x}_0 \quad \text{and} \quad \mathbf{x} = \mathbf{x}_0 \pm \frac{\delta}{2}\mathbf{n}. \tag{20}$$

With eqn (19), we first obtain

$$\nabla \cdot \dot{\mathbf{s}} = \nabla \cdot \dot{\mathbf{s}}_c + f'(n)[[\dot{\mathbf{t}}]], \tag{21}$$

where $f'(n) = \partial f/\partial n$ and where the jump in the total traction rate $[[\dot{\mathbf{t}}]]$ is defined as

$$[[\dot{\mathbf{t}}]] = \dot{\mathbf{t}}_{(b)} - \dot{\mathbf{t}}_{c(b)} = \mathbf{n} \cdot [[\mathbf{E}]] : \dot{\boldsymbol{\varepsilon}}_{c(b)} + \frac{1}{\delta}\mathbf{Q}_{(b)} \cdot [[\dot{\mathbf{u}}]] - [[\dot{p}]]\mathbf{n} \tag{22}$$

with $\dot{\mathbf{t}}_{(b)} = \mathbf{n} \cdot \dot{\mathbf{s}}(\mathbf{x}_0)$ and $\dot{\mathbf{t}}_{c(b)} = \mathbf{n} \cdot \dot{\mathbf{s}}_c(\mathbf{x}_0)$. In eqn (22), $\mathbf{Q}_{(b)}$ is the acoustic tensor associated with $\mathbf{E}_{(b)}$ in the band. Clearly, $\mathbf{Q}_{(b)}$ will assume the value $\mathbf{Q}^{ep}$ or $\mathbf{Q}^{e}$ depending on whether plastic loading or elastic unloading takes place in this band, as determined by $\dot{\boldsymbol{\varepsilon}}_{(b)}$ according to the loading condition $(16a)_1$. As usual, cf. Ottosen and Runesson (1991), $\mathbf{Q}^e$ and $\mathbf{Q}^{ep}$ are given as

$$\mathbf{Q}^e = \mathbf{n} \cdot \mathbf{E}^e \cdot \mathbf{n}, \quad \mathbf{Q}^{ep} = \mathbf{n} \cdot \mathbf{E}^{ep} \cdot \mathbf{n} = \mathbf{Q}^e - \frac{1}{h}\mathbf{b}\mathbf{a}. \tag{23}$$

Now, upon using a simple difference scheme for calculating $f'(n)$, we obtain $f'(0) = 0$, $f'(\pm\delta/2) = \mp 1/\delta$. Combining eqn (20) with eqn (22), we then conclude that the momentum conservation requires that

$$[[\dot{\mathbf{t}}]] = 0 \quad \text{or} \quad \dot{\mathbf{t}}_{(b)} = \dot{\mathbf{t}}_{c(b)} = 0, \tag{24a}$$

i.e. the total traction rate is continuous across the band. With eqn (22), we may rewrite eqn (24) more explicitly as

$$\frac{1}{\delta}\mathbf{Q}_{(b)} \cdot [[\dot{\mathbf{u}}]] - [[\dot{p}]]\mathbf{n} = -\mathbf{n} \cdot [[\mathbf{E}]] : \dot{\boldsymbol{\varepsilon}}_{c(b)}. \tag{24b}$$

Remark. This is the classical requirement for localization put in a slightly different context. The corresponding "drained" version, i.e. without any pore pressure augmentation, was given by Larsson and Runesson (1995). ●

3.3. *Mass balance*

In this paper we shall restrict the analysis to the fully undrained situation defined by $\nabla \cdot v = 0$. Conservation of mass inside, as well as outside, the band then requires that

$$-\dot{\varepsilon}_v + \dot{\varepsilon}_v^{\mathrm{f}} = 0 \quad \text{for } \mathbf{x} = \mathbf{x}_0 \quad \text{and} \quad \mathbf{x} = \mathbf{x}_0 + \frac{\delta}{2}\mathbf{n}. \tag{25}$$

With eqns (6), (14b) and (18), we conclude that

$$-\dot{\varepsilon}_v + \dot{\varepsilon}_v^{\mathrm{f}} = -\dot{\varepsilon}_{v,\mathrm{c}} - \frac{1}{K^{\mathrm{f}}}\dot{p}_{\mathrm{c}} - \frac{f(n)}{\delta}\mathbf{n} \cdot [[\dot{\mathbf{u}}]] - \frac{f(n)}{K^{\mathrm{f}}}[[\dot{p}]]. \tag{26}$$

Upon combining eqn (25) with eqn (26), while utilizing the continuity of $\dot{\boldsymbol{\varepsilon}}_{\mathrm{c}}$ and $\dot{p}_{\mathrm{c}}$, we conclude that the preserved mass balance across the band requires that

$$\frac{1}{\delta}\mathbf{n} \cdot [[\dot{\mathbf{u}}]] + \frac{1}{K^{\mathrm{f}}}[[\dot{p}]] = 0. \tag{27}$$

Finally, we combine the momentum and mass balance equations (24b) and (27) to obtain

$$S[[\dot{p}]] = B, \tag{28}$$

where

$$S = \mathbf{n} \cdot \mathbf{P}_{(\mathrm{b})} \cdot \mathbf{n} + \frac{1}{K^{\mathrm{f}}}, \quad B = (\mathbf{n} \cdot \mathbf{P}_{(\mathrm{b})}) \cdot (\mathbf{n} \cdot [[\mathbf{E}]] : \dot{\boldsymbol{\varepsilon}}_{\mathrm{c(b)}}), \quad \mathbf{P}_{(\mathrm{b})} = (\mathbf{Q}_{\mathrm{b}})^{-1}. \tag{29}$$

On the other hand, provided that $K^{\mathrm{f}} < \infty$, we may eliminate $[[\dot{p}]]$ to obtain the condition

$$\frac{1}{\delta}\mathbf{Q}^{\mathrm{u}}_{(\mathrm{b})} \cdot [[\dot{\mathbf{u}}]] = -\mathbf{n} \cdot [[\mathbf{E}]] : \dot{\boldsymbol{\varepsilon}}_{\mathrm{c(b)}}, \tag{30}$$

where $\mathbf{Q}^{\mathrm{u}}_{\mathrm{b}}$ is the "undrained" acoustic tensor defined as

$$\mathbf{Q}^{\mathrm{u}}_{(\mathrm{b})} = \mathbf{Q}_{(\mathrm{b})} + K^{\mathrm{f}}\mathbf{n}\mathbf{n} \tag{31}$$

as introduced by Runesson *et al.* (1995).

3.4. *Conditions for onset of localization*

We investigate the implications of the localization condition in the form eqns (28) and (30). To this end, we consider three different cases, depending on the actual loading condition, (*P*) or (*E*), in Ω^{b} and $\Omega^{\pm}$ at the onset of localization.

Case 1. Elastic unloading (*E*) is assumed in Ω^{b} as well as in $\Omega^{\pm}$. With $\mathbf{E}_{(\mathrm{b})} = \mathbf{E}_{\mathrm{c(b)}} = \mathbf{E}^{\mathrm{e}}$, we obtain from eqns (28) and (30) the pertinent equations

$$S^{\mathrm{e}}[[\dot{p}]] = 0, \quad S^{\mathrm{e}} = \mathbf{n} \cdot \mathbf{P}^{\mathrm{e}} \cdot \mathbf{n} + \frac{1}{K^{\mathrm{f}}} \tag{32}$$

$$\frac{1}{\delta}\mathbf{Q}^{\mathrm{u,e}} \cdot [[\dot{\mathbf{u}}]] = 0, \quad \mathbf{Q}^{\mathrm{u,e}} = \mathbf{Q}^{\mathrm{e}} + K^{\mathrm{f}}\mathbf{n}\mathbf{n}. \tag{33}$$

Since $\mathbf{P}^{e}$ (and $\mathbf{Q}^{e}$) are positive definite, and $K^{f} > 0$, we conclude that $S^{e} > 0$ and $\mathbf{Q}^{u,e}$ is positive definite. Hence, the only solution is $[[\dot{p}]] = 0$ and $[[\dot{\mathbf{u}}]] = \mathbf{0}$.

Case 2. Plastic loading (P) is assumed in Ω^{b} as well as in $\Omega^{\pm}$. With $\mathbf{E}_{(b)} = \mathbf{E}_{c(b)} = \mathbf{E}^{ep}$, we obtain the equations

$$S^{ep}[[\dot{p}]] = 0, \quad S^{ep} = \mathbf{n}\cdot\mathbf{P}^{ep}\cdot\mathbf{n} + \frac{1}{K^{f}} \tag{34}$$

$$\frac{1}{\delta}\mathbf{Q}^{u,ep}\cdot[[\dot{\mathbf{u}}]] = 0, \quad \mathbf{Q}^{u,ep} = \mathbf{Q}^{ep} + K^{f}\mathbf{nn}. \tag{35}$$

It appears that necessary conditions for the existence of non-trivial solutions $[[\dot{p}]] \neq 0$ and $[[\dot{\mathbf{u}}]] \neq \mathbf{0}$ are that $S^{ep} = 0$ and $\mathbf{Q}^{u,ep}$ is singular, respectively. It can be shown, Runesson *et al.* (1995), that these singularity conditions are identical. In order to be more complete, we shall recall some spectral properties derived originally by Runesson *et al.* (1995):

Using the Sherman–Morrison formula, we may express $\mathbf{P}^{ep} = (\mathbf{Q}^{ep})^{-1}$ explicitly as

$$\mathbf{P}^{ep} = \mathbf{P}^{e} + \frac{1}{h - \mathbf{a}\cdot\mathbf{P}^{e}\cdot\mathbf{b}}\mathbf{P}^{e}\cdot\mathbf{ba}\cdot\mathbf{P}^{e}. \tag{36}$$

By invoking eqn (36) into eqn (34b), we obtain the condition for "undrained" singularity of S^{ep} (or $\mathbf{Q}^{u,ep}$) as $h = h_u$ with h_u given by

$$h_u = \mathbf{a}\cdot\mathbf{P}^{e}\cdot\mathbf{b} - \Psi\frac{(\mathbf{n}\cdot\mathbf{P}^{e}\cdot\mathbf{b})(\mathbf{a}\cdot\mathbf{P}^{e}\cdot\mathbf{n})}{\mathbf{n}\cdot\mathbf{P}^{e}\cdot\mathbf{n}}, \quad \Psi = \frac{K^{f}\mathbf{n}\cdot\mathbf{P}^{e}\cdot\mathbf{n}}{1 + K^{f}\mathbf{n}\cdot\mathbf{P}^{e}\cdot\mathbf{n}}. \tag{37}$$

The two extremes $\Psi = 0$ (or $K^{f} = 0$) and $\Psi = 1$ (or $K^{f} = \infty$) correspond to empty pores (one-phase material) and incompressible pore fluid, respectively. It follows readily from eqn (37) that $h_u = h_d$ when $\Psi = 0$, with

$$h_d = \mathbf{a}\cdot\mathbf{P}^{e}\cdot\mathbf{b}. \tag{38}$$

cf. Ottosen and Runesson (1991), whereas the maximal difference between h_d and h_u is encountered when $\Psi = 1$. Under the mild restriction that $sign(\mathbf{a}\cdot\mathbf{P}^{e}\cdot\mathbf{n}) = sign(\mathbf{b}\cdot\mathbf{P}^{e}\cdot\mathbf{n})$, it follows that $h_u \leqslant h_d$, i.e. the "undrained" singularity condition is satisfied later (for smaller hardening modulus) than the "drained".

We may now conveniently introduce the reduced moduli $\bar{H}_u = H - H_u$ and $\bar{H}_d = H - H_d$ (for given value of H). Upon combining eqns (37) and (38), and inserting into eqn (36), we may rewrite $\mathbf{P}^{ep}$ as

$$\begin{aligned}\mathbf{P}^{ep} &= \mathbf{P}^{e} + \frac{1}{\bar{H}_d}\mathbf{P}^{e}\cdot\mathbf{ba}\cdot\mathbf{P}^{e} \\ &= \mathbf{P}^{e} + \frac{\mathbf{n}\cdot\mathbf{P}^{e}\cdot\mathbf{n}}{\bar{H}_u\mathbf{n}\cdot\mathbf{P}^{e}\cdot\mathbf{n} - \Psi(\mathbf{n}\cdot\mathbf{P}^{e}\cdot\mathbf{b})(\mathbf{a}\cdot\mathbf{P}^{e}\cdot\mathbf{n})}\mathbf{P}^{e}\cdot\mathbf{ba}\cdot\mathbf{P}^{e}.\end{aligned} \tag{39}$$

By invoking the localization criterion $\bar{H}_u = 0$ (for any value of $\mathbf{n}$), we may use eqns (39) and (24b) to obtain the result

$$[[\dot{\mathbf{u}}]] = \delta[[\dot{p}]]\mathbf{P}^{\mathrm{ep}}\cdot\mathbf{n} \equiv \delta[[\dot{p}]]\mathbf{P}^{\mathrm{e}}\cdot\mathbf{w}, \quad \mathbf{w} = \mathbf{n} - \frac{\mathbf{n}\cdot\mathbf{P}^{\mathrm{e}}\cdot\mathbf{n}}{\Psi\mathbf{n}\cdot\mathbf{P}^{\mathrm{e}}\cdot\mathbf{b}}\mathbf{b}. \tag{40}$$

Remark. It can be shown, Runesson *et al.* (1995), that $\mathbf{w}$ is the eigenvector to $\mathbf{Q}^{\mathrm{u,ep}}$ corresponding to the smallest eigenvalue μ_{u} in elastic metric, i.e.

$$\mathbf{Q}^{\mathrm{u,ep}}\cdot\mathbf{w} = \mu_{\mathrm{u}}\mathbf{Q}^{\mathrm{e}}\cdot\mathbf{w}. \tag{41}$$

Moreover, we may express S^{ep} as

$$S^{\mathrm{ep}} = \frac{\bar{H}_{\mathrm{u}}(\mathbf{n}\cdot\mathbf{P}^{\mathrm{e}}\cdot\mathbf{n})^2}{\Psi(\bar{H}_{\mathrm{u}}\mathbf{n}\cdot\mathbf{P}^{\mathrm{e}}\cdot\mathbf{n} - \Psi(\mathbf{n}\cdot\mathbf{P}^{\mathrm{e}}\cdot\mathbf{b})(\mathbf{a}\cdot\mathbf{P}^{\mathrm{e}}\cdot\mathbf{n}))}. \tag{42}$$

Case 3. Plastic loading (P) is assumed in Ω^{b}, whereas elastic unloading is assumed in $\Omega^{\pm}$. With $\mathbf{E}_{(\mathrm{b})} = \mathbf{E}^{\mathrm{ep}}$ and $\mathbf{E}_{\mathrm{c(b)}} = \mathbf{E}^{\mathrm{e}}$, we obtain

$$S^{\mathrm{ep}}[[\dot{p}]] = -\dot{\lambda}_{\mathrm{c}}\mathbf{n}\cdot\mathbf{P}^{\mathrm{ep}}\cdot\mathbf{b} = -\dot{\lambda}_{\mathrm{c}}\frac{h(\mathbf{n}\cdot\mathbf{P}^{\mathrm{e}}\cdot\mathbf{b})(\mathbf{n}\cdot\mathbf{P}^{\mathrm{e}}\cdot\mathbf{n})}{\bar{H}_{\mathrm{u}}\mathbf{n}\cdot\mathbf{P}^{\mathrm{e}}\cdot\mathbf{n} - \Psi(\mathbf{n}\cdot\mathbf{P}^{\mathrm{e}}\cdot\mathbf{b})(\mathbf{a}\cdot\mathbf{P}^{\mathrm{e}}\cdot\mathbf{n})} \tag{43}$$

$$\frac{1}{\delta}\mathbf{Q}^{\mathrm{u,ep}}\cdot[[\dot{\mathbf{u}}]] = \dot{\lambda}_{\mathrm{c}}\mathbf{b} \tag{44}$$

with

$$\dot{\lambda}_{\mathrm{c}} = \frac{1}{h}\mathbf{f}:\mathbf{E}^{\mathrm{e}}:\dot{\boldsymbol{\varepsilon}}_{\mathrm{c(b)}} \leqslant 0. \tag{45}$$

The solution of $[[\dot{p}]]$ is obtained from eqn (43) and eqn (42) as

$$[[\dot{p}]] = -\frac{\dot{\lambda}_{\mathrm{c}}h\Psi\mathbf{n}\cdot\mathbf{P}^{\mathrm{e}}\cdot\mathbf{b}}{\bar{H}_{\mathrm{u}}\mathbf{n}\cdot\mathbf{P}^{\mathrm{e}}\cdot\mathbf{n}}. \tag{46}$$

Upon inserting eqn (46) into eqn (24b), it appears that the localization mode $[[\dot{\mathbf{u}}]]$ is given by

$$[[\dot{\mathbf{u}}]] = -\frac{\delta\dot{\lambda}_{\mathrm{c}}h\Psi\mathbf{n}\cdot\mathbf{P}^{\mathrm{e}}\cdot\mathbf{b}}{\bar{H}_{\mathrm{u}}\mathbf{n}\cdot\mathbf{P}^{\mathrm{e}}\cdot\mathbf{n}}\mathbf{P}^{\mathrm{e}}\cdot\mathbf{w}, \tag{47}$$

where $\mathbf{w}$ was given in eqn $(40)_2$.

Next, we consider the validity of the solution (47) on the basis of the assumed loading condition in Ω^b and $\Omega_{\mathrm{c}}^{\pm}$, respectively. The assumptions about unloading in $\Omega^{\pm}$ gives $\dot{\lambda}_{\mathrm{c}} < 0$, whereas the condition of plastic loading in Ω^b can be rewritten

$$\dot{\lambda}_{\mathrm{c}} + \frac{1}{\delta h}\mathbf{a}\cdot[[\dot{\mathbf{u}}]] = \frac{\dot{\lambda}_{\mathrm{c}}h}{\bar{H}_{\mathrm{u}}} > 0 \quad \text{in} \quad \Omega^b. \tag{48}$$

It thus follows that the assumption about plastic loading in Ω^b can be satisfied only if $\bar{H}_{\mathrm{u}} < 0$, i.e. $H < H_{\mathrm{u}}$, which requires a discontinuous change of H at the state where band-shaped localization becomes possible.

Remark. In the special case of neutral loading in $\Omega^{\pm}$, i.e. $\dot{\lambda}_{\mathrm{c}} = 0$, then two different situations must be distinguished: the first situation is that $\bar{H}_{\mathrm{u}} \neq 0$, whereby it follows from eqns (46) and (47) that $[[\dot{p}]] = 0$ and $[[\dot{\mathbf{u}}]] = \mathbf{0}$. The second situation is that $\bar{H}_u = 0$, whereby it follows that the magnitudes of $[[\dot{p}]]$ and $[[\dot{\mathbf{u}}]]$ are undetermined. It appears that this situation is, in fact, represented by Case 2.●

In conclusion, we have shown the following results for the onset of localization:

(a) The condition for localization pertinent to completely undrained behavior is satisfied when the hardening modulus achieves the value $H = H_{u,cr}$.

(b) The orientation $\mathbf{n} = \mathbf{n}_{cr}$ of the "undrained localization band" is defined by the state when $H = H_{u,cr}$ (or $S^{ep} = 0$).

(c) Band-shaped localization, in the sense of a developing plastic band (whereas elastic unloading takes place outside the band) is not possible unless $H < H_{u,cr}$ (or $S^{ep} < 0$), i.e. a discontinuous change of H at the onset of localization is required.

3.5. *A remark on post-localized behavior*

The earliest possibility for localization is defined (in the usual way) by

$$\mathbf{n}_{cr} = \arg(|\mathbf{n}| \overset{\max}{=} 1\, h_u(\mathbf{n})) \tag{49}$$

with $h_u(\mathbf{n})$ given in eqn (37). Analytical solutions were given by Runesson *et al.* (1995). In particular, the surprising result that the shear band should be expected to be oriented 45° to one principal stress direction was obtained. This result holds for quite a large class of isotropic elastic–plastic materials with non-associated plastic flow rule.

In the post-localized range, the band-orientation is held fixed in accordance with eqn (49). This strategy is analogous with the treatment of brittle materials, where localization is rather interpreted as macro-cracks. Moreover, the softening modulus H has a well-defined meaning only in a distributional sense as soon as the shear band starts to develop. Hence, the proper value of H will depend on the regularization parameter δ in such a fashion that the "right", *a priori* given, energy is dissipated within the chosen calibration mode, cf. the fictitious "crack" approach for brittle materials, as discussed by Larsson and Runesson (1995). We then conclude that the only difference between semi-brittle and ductile behavior is the amount of plastic deformation that precedes the localization event. Clearly, the extreme case (which is pertinent to brittle fracture) is that localization occurs at the very onset of plastic yielding.

Remark. We have assumed undrained behavior at the explicit analysis, which is a useful approximation in the case that the permeability is small and/or the loading rate is large. In such a case the behavior is rate-independent and there is no time-scale in the problem. The more complex situation of partly drained behavior (of a consolidating soil) due to a finite permeability in the pre-localized as well as post-localized regime, is a subject of a forthcoming paper. Here we merely note that the general situation was discussed by Rudnicki (1983); however, without reference to regularized discontinuous displacements.●

4. MIXED VARIATIONAL FORMULATION WITH EMBEDDED DISCONTINUITY

In this section we propose a mixed variational formulation, where the corresponding finite element discretization can be constructed in such a way that nodal values represent continuous (=compatible) portions of the displacement and pore pressure fields. In order to arrive at the appropriate variational formulation, we resort to the "enhanced strain" approach, Simo and Rifai (1990), that is extended to include regularized strain discontinuities. The present developments are made in the spirit of the developments in Larsson and Runesson (1995), where, in particular, the strain is expressed in terms of a compatible and an incompatible portion defined as

$$\boldsymbol{\varepsilon}' = \boldsymbol{\varepsilon}'_c + \tilde{\boldsymbol{\varepsilon}}', \quad \tilde{\boldsymbol{\varepsilon}}' = \tilde{\boldsymbol{\varepsilon}}'_c + \frac{f(n)}{2\delta}(\mathbf{n}[[\tilde{\mathbf{u}}']] + [[\tilde{\mathbf{u}}']]\mathbf{n}). \tag{50}$$

Moreover, in order to invoke a regularized pore pressure discontinuity, we introduce the pore pressure field, in a similar fashion as the strain field, as

$$p' = p'_c + \tilde{p}', \quad \tilde{p}' = \tilde{p}'_c + f(n)[[\tilde{p}']]. \tag{51}$$

The three-field variational formulation with equilibrium, kinematics and the constitutive relations becomes

$$\int_\Omega \boldsymbol{\varepsilon}'_c : \boldsymbol{\tau}\, d\Omega - W^{ext}_u(\mathbf{u}'_c) = 0 \quad \forall \mathbf{u}'_c \in V_c \tag{52a}$$

$$\int_\Omega \boldsymbol{\tau}' : (\boldsymbol{\varepsilon}_c - \boldsymbol{\varepsilon})\, d\Omega = 0 \quad \forall \boldsymbol{\tau}' \in S \tag{52b}$$

$$\int_\Omega \boldsymbol{\varepsilon}' : (-\boldsymbol{\tau} + \boldsymbol{\sigma}(\boldsymbol{\varepsilon}) - p\boldsymbol{\delta})\, d\Omega = 0 \quad \forall \boldsymbol{\varepsilon}' \in E, \tag{52c}$$

where the solution $(\mathbf{u}_c, \boldsymbol{\tau}, \boldsymbol{\varepsilon})$ belongs to the class of functions $V_c \times S \times E$. Here, V_c is the usual space of compatible (in particular continuous) displacements $\mathbf{u}_c$, and the function space S contains square integrable stresses $\boldsymbol{\tau}$. As to the strain space E, we use the structure of the strain introduced in eqn (50) to propose that $\boldsymbol{\varepsilon}' \in E$ is defined as

$$\boldsymbol{\varepsilon}' = \boldsymbol{\varepsilon}'_c + \tilde{\boldsymbol{\varepsilon}}', \quad \tilde{\boldsymbol{\varepsilon}}' \in \tilde{E}. \tag{53}$$

Upon inserting eqn (53) into eqn (52a, b, c), we conclude that eqn (52) can be rephrased as

$$\int_\Omega \boldsymbol{\varepsilon}'_c : (\boldsymbol{\sigma}(\boldsymbol{\varepsilon}) - p\boldsymbol{\delta})\, d\Omega - W^{ext}_u(\mathbf{u}'_c) = 0 \quad \forall \mathbf{u}'_c \in V_c \tag{54a}$$

$$\int_\Omega \boldsymbol{\tau}' : \tilde{\boldsymbol{\varepsilon}}\, d\Omega = 0 \quad \forall \boldsymbol{\tau}' \in S \tag{54b}$$

$$\int_\Omega \tilde{\boldsymbol{\varepsilon}}' : (-\boldsymbol{\tau} + \boldsymbol{\sigma}(\boldsymbol{\varepsilon}) - p\boldsymbol{\delta})\, d\Omega = 0 \quad \forall \tilde{\boldsymbol{\varepsilon}}' \in \tilde{E}. \tag{54c}$$

The three-field variational formulation associated with mass balance, pore-pressure and kinematics is proposed as follows:

$$-\int_\Omega p'_c \dot{\gamma}_v\, d\Omega - W^{ext}_p(p'_c) = 0 \quad \forall p'_c \in P_c \tag{55a}$$

$$\int_\Omega \gamma'_v (p_c - p)\, d\Omega = 0 \quad \forall \gamma'_v \in E_v \tag{55b}$$

$$\int_\Omega p' \cdot \left(-\dot{\gamma}_v + \dot{\varepsilon}_v + \frac{1}{K^f}\dot{p} \right) d\Omega = 0 \quad \forall p' \in P, \tag{55c}$$

where the solution (p, γ_v), belongs to the class of functions $P \times E_v$. Here, E_v contains square integrable volumetric strains γ_v. With regard to the space P of pore pressures, we propose that

$$p' = p'_c + \tilde{p}', \quad \tilde{p}' \in \tilde{P}. \tag{56}$$

Upon inserting eqn (56) into eqn (55a, b, c), we conclude that these equations can be rewritten as

$$-\int_{\Omega} p_c'\left(\dot{\varepsilon}_v+\frac{1}{K^f}\dot{p}\right)\mathrm{d}\Omega - W_p^{\mathrm{ext}}(p_c') = 0 \quad \forall p_c' \in P_c \tag{57a}$$

$$\int_{\Omega} \gamma_v'\tilde{p}\,\mathrm{d}\Omega = 0 \quad \forall \gamma_v' \in E_v \tag{57b}$$

$$-\int_{\Omega} \tilde{p}'\left(-\dot{\gamma}_v+\dot{\varepsilon}_v+\frac{1}{K^f}\dot{p}\right)\mathrm{d}\Omega = 0 \quad \forall \tilde{p}' \in \tilde{P}. \tag{57c}$$

Let us next choose $(S, \tilde{E})$ and $(E_v, \tilde{P})$ mutually orthogonal in $L_2(\Omega)$, respectively. We thus obtain the orthogonality conditions

$$\int_{\Omega} \boldsymbol{\tau}' : \tilde{\boldsymbol{\varepsilon}}'\,\mathrm{d}\Omega \equiv 0, \quad \forall \boldsymbol{\tau}' \in S, \quad \forall \tilde{\boldsymbol{\varepsilon}}' \in \tilde{E} \tag{58}$$

$$\int_{\Omega} \gamma_v'\tilde{p}'\,\mathrm{d}\Omega \equiv 0, \quad \forall \gamma_v' \in E_v, \quad \forall \tilde{p}' \in \tilde{P}. \tag{59}$$

We now conclude that eqns (54b) and (57b) are identically satisfied. This means that the stress field $\boldsymbol{\tau} \in S$ and the volumetric strain field $\gamma_v \in E_v$ may be eliminated in eqns (54c) and (57c), respectively.

Hence, we may rephrase the equilibrium equation (54) as

$$\int_{\Omega} \boldsymbol{\varepsilon}_c' : (\boldsymbol{\sigma}(\boldsymbol{\varepsilon}) - p\boldsymbol{\delta})\,\mathrm{d}\Omega - W_u^{\mathrm{ext}}(u_c') = 0, \quad \forall u_c' \in V_c \tag{60a}$$

$$\int_{\Omega} \tilde{\boldsymbol{\varepsilon}}' : (\boldsymbol{\sigma}(\boldsymbol{\varepsilon}) - p\boldsymbol{\delta})\,\mathrm{d}\Omega = 0, \quad \forall \tilde{\boldsymbol{\varepsilon}}' \in \tilde{E}, \tag{60b}$$

where, in the present context, $\boldsymbol{\sigma} := {}^{n+1}\boldsymbol{\sigma}({}^{n+1}\boldsymbol{\varepsilon})$ is the solid stress that is obtained from integration of the constitutive relations.

The mass balance equation (57) is written analogously as

$$-\int_{\Omega} p_c'\left(\varepsilon_v+\frac{1}{K^f}p\right)\mathrm{d}\Omega = W_p^{\mathrm{ext}}(p_c') \quad \forall p_c' \in P_c \tag{61a}$$

$$-\int_{\Omega} \tilde{p}'\left(\varepsilon_v+\frac{1}{K^f}p\right)\mathrm{d}\Omega = 0 \quad \forall \tilde{p}' \in \tilde{P}, \tag{61b}$$

which represent the integrated form of eqn (57a, c). It is noted that the variables are updated values at a certain time-step.

From eqns (60) and (61), we note that eqns (60a) and (61a) constitute a set of coupled global equilibrium and continuity equations, whereas eqns (60b) and (61b) are the corresponding (local) *projection problems*, denoted $\Pi_\varepsilon(\Omega)$ and $\Pi_p(\Omega)$ subsequently.

5. FINITE ELEMENT FORMULATION

5.1. *FE-approximation pertinent to an enhanced CST-element*

We consider the region Ω discretized into NEL finite elements Ω_e, $e = 1, \ldots, NEL$. In order to construct the simplest possible augmentation of the CST-element to represent undrained behavior, we assume that p_c is piecewise constant (in each element Ω_e). The element approximation may be written in matrix form as

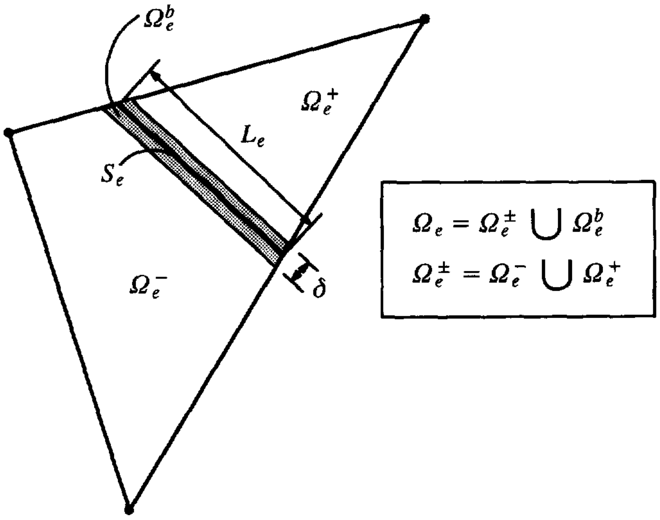

Fig. 2. Enhanced constant strain triangle with embedded localization band.

$$\mathbf{u}_c = \mathbf{N}_e \mathbf{u}_e, \quad \boldsymbol{\varepsilon}_c = \mathbf{B}_e \mathbf{u}_e, \quad p_c = p_e, \tag{62}$$

where the matrix $\mathbf{N}_e$ contains the standard compatible shape functions, whereas $\mathbf{B}_e$ is the strain-displacement matrix.

As to stress and strain interpolation, the stresses $\boldsymbol{\tau} \in S$ and the enhanced strain $\tilde{\boldsymbol{\varepsilon}} \in \tilde{E}$ are chosen as piecewise constant (within each Ω_e) such that

$$\boldsymbol{\tau} = \sum_{e=1}^{NEL} \chi_e \boldsymbol{\tau}_e, \quad \tilde{\boldsymbol{\varepsilon}}_c = \sum_{e=1}^{NEL} \chi_e \tilde{\boldsymbol{\varepsilon}}_{ce}, \quad [[\tilde{\mathbf{u}}]] = \sum_{e=1}^{NEL} \chi_e [[\tilde{\mathbf{u}}]]_e, \tag{63}$$

where χ_e is defined as

$$\chi_e = \begin{cases} 1 & \text{iff } x \in \Omega_e \\ 0 & \text{otherwise.} \end{cases} \tag{64}$$

We also introduce the following piecewise constant fields:

$$\gamma_v = \sum_{e=1}^{NEL} \chi_e \gamma_{ve}, \quad \tilde{p}_c = \sum_{e=1}^{NEL} \chi_e \tilde{p}_{ce}, \quad [[\tilde{p}]] = \sum_{e=1}^{NEL} \chi_e [[\tilde{p}]]_e. \tag{65}$$

Upon inserting these FE-approximations into the "orthogonality" conditions (58) and (59), that must be satisfied for each element $e = 1, \ldots, NEL$, we obtain

$$\tilde{\boldsymbol{\varepsilon}}'_{ce} = -\frac{1}{2l_e}(\mathbf{n}[[\tilde{\mathbf{u}}']]_e + [[\tilde{\mathbf{u}}']]_e \mathbf{n}) \tag{66a}$$

$$\tilde{p}'_{ce} = -\frac{\delta}{l_e}[[\tilde{p}']]_e, \tag{66b}$$

where $l_e = A_e/L_e$, $A_e = m(\Omega_e)$ and $L_e = m(S_e)$, cf. Fig. 2. It was also assumed that $\mathbf{n}$ is constant.

In summary, we may express the discretized fields in matrix notation as follows:

$$\boldsymbol{\varepsilon} = \mathbf{B}_e\mathbf{u}_e + \frac{1}{\delta}\left(f(n) - \frac{\delta}{l_e}\right)\mathbf{C}_e[[\tilde{\mathbf{u}}]]_e \tag{67a}$$

$$p = p_e + \left(f(n) - \frac{\delta}{l_e}\right)[[\tilde{p}]]_e. \tag{67b}$$

Since all fields are element wise constant, we may (without risking any confusion) label $\boldsymbol{\varepsilon}_e$ as $\boldsymbol{\varepsilon}_\mathrm{b}$ when $\mathbf{x}\in\Omega_e^\mathrm{b}$ and $\boldsymbol{\varepsilon}_e$ as $\boldsymbol{\varepsilon}_\mathrm{c}$ when $\mathbf{x}\in\Omega_e^\pm$. Moreover in eqn (67a), we have introduced $\mathbf{C}_e[[\tilde{\mathbf{u}}]]_e$ as the matrix representation of the tensor $(\mathbf{n}[[\tilde{\mathbf{u}}]]_e + [[\tilde{\mathbf{u}}]]_e\mathbf{n})/2$. This means, for example, that the matrix equivalent of $\mathbf{n}\cdot\boldsymbol{\sigma}$ is $\mathbf{C}_e^\mathrm{T}\boldsymbol{\sigma}$.

5.2. *FE-equations*

Let us return to the (global) equilibrium equation (60a) restated as

$$\sum_{e=1}^{NEL}\left(\int_{\Omega_e}\boldsymbol{\varepsilon}_\mathrm{c}' : (\boldsymbol{\sigma}(\boldsymbol{\varepsilon}) - p\boldsymbol{\delta})\right)\mathrm{d}\Omega = \sum_{e=1}^{NEL} W_{\mathrm{u},e}^{\mathrm{ext}}(\mathbf{u}_\mathrm{c}'), \tag{68}$$

where (due to the assumption about constant strain and pressure) the integration can be carried out explicitly within each Ω_e to give

$$\sum_{e=1}^{NEL}\left(A_e\left(1 - \frac{\delta}{l_e}\right)\boldsymbol{\varepsilon}_\mathrm{c}' : \boldsymbol{\sigma}_\mathrm{c} + A_e\frac{\delta}{l_e}\boldsymbol{\varepsilon}_\mathrm{c}' : \boldsymbol{\sigma}_\mathrm{b} - A_e\varepsilon_{\mathrm{cv}}' p_e\right) = \sum_{e=1}^{NEL} W_{\mathrm{u},e}^{\mathrm{ext}}(\mathbf{u}_\mathrm{c}'). \tag{69}$$

Here, it was used that

$$\int_{\Omega_e}\varepsilon_{\mathrm{cv}}'\left(f(n) - \frac{\delta}{l_e}\right)\mathrm{d}\Omega = 0, \tag{70}$$

which effectively excludes the pore pressure discontinuity from the global equilibrium equation.

Upon writing $\varepsilon_{\mathrm{cv}}$ as $\mathbf{B}_{ve}u_e$, we may give eqn (69) in matrix format as

$$\mathop{\mathbf{A}}_{e=1}^{NEL}\mathbf{g}_e = \mathop{\mathbf{A}}_{e=1}^{NEL}[\mathbf{b}_e - \mathbf{f}_e^{\mathrm{ext}}] = \mathbf{0}, \tag{71}$$

where the internal element forces are defined as

$$\mathbf{b}_e = A_e\left(1 - \frac{\delta}{l_e}\right)\mathbf{B}_e^\mathrm{T}\boldsymbol{\sigma}_\mathrm{c} + A_e\frac{\delta}{l_e}\boldsymbol{\sigma}_\mathrm{b} - A_e\mathbf{B}_{ve}^\mathrm{T}p_e. \tag{72}$$

In this expression, it is emphasized that p_e is the scalar pore pressure, which can be resolved at the element level, as discussed subsequently.

Next, we consider the projection problem $\Pi_\varepsilon(\Omega)$ in eqn (60b), which with eqn (67a) can be rewritten as

$$\int_{\Omega_e}\frac{1}{\delta}\left(f(n) - \frac{\delta}{l_e}\right)[[\tilde{u}']]_e\cdot(\mathbf{n}\cdot\boldsymbol{\sigma})\,\mathrm{d}\Omega - \int_{\Omega_e}\frac{1}{\delta}\left(f(n) - \frac{\delta}{l_e}\right)[[\tilde{\mathbf{u}}']]_e\cdot\mathbf{n}p_e\,\mathrm{d}\Omega = \mathbf{0}. \tag{73}$$

Upon invoking also p_e, from eqn (67b) into eqn (73), we obtain

$$\frac{A_e}{l_e}\left(1-\frac{\delta}{l_e}\right)[[\tilde{\mathbf{u}}']]_e\cdot(-\mathbf{n}\cdot\boldsymbol{\sigma}_c+\mathbf{n}\cdot\boldsymbol{\sigma}_b-\mathbf{n}[[\tilde{p}]]_e)=\mathbf{0}, \tag{74}$$

where it was used that

$$\int_{\Omega_e}\frac{1}{\delta}p_c\left(f(n)-\frac{\delta}{l_e}\right)\mathrm{d}\Omega=0. \tag{75}$$

The relation (73) must be valid for all elements, which is written in matrix notation as

$$\mathbf{x}_e=\frac{A_e}{l_e}\left(1-\frac{\delta}{l_e}\right)(-\mathbf{C}_e^{\mathrm{T}}\boldsymbol{\sigma}_c+\mathbf{C}_e^{\mathrm{T}}\boldsymbol{\sigma}_b-\mathbf{n}[[\tilde{p}]]_e)=\mathbf{0}\quad e=1,2,\ldots NEL. \tag{76}$$

Remark. The local projection problem (76) ensures that the (total) traction vector is continuous across S_e, i.e. $\mathbf{t}=\mathbf{0}$. This feature of the projection problem was also pointed out by Larsson and Runesson (1995) for the fully drained continuum.●

As to the mass balance equation, we may simplify the global relation (61a) to

$$\sum_{e=1}^{NEL}\left(-\int_{\Omega}p_c'\left(\varepsilon_v+\frac{1}{K^{\mathrm{f}}}p\right)\mathrm{d}\Omega\right)=\sum_{e=1}^{NEL}W_{\mathrm{p},e}^{\mathrm{ext}}(p_c'). \tag{77}$$

Upon introducing ε_{ve} and p_e, as defined by eqn (66ab), it is noted (like for the equilibrium equation) that the enhanced portions vanish at the global level. Consequently, eqn (77) becomes

$$\sum_{e=1}^{NEL}\left(-A_e p_c'\left(\varepsilon_{vc}+\frac{1}{K^{\mathrm{f}}}p_c\right)\mathrm{d}\Omega\right)=\sum_{e=1}^{NEL}W_{\mathrm{p},e}^{\mathrm{ext}}(p_c'). \tag{78}$$

Since p_e is defined only at the elemental level, we note that eqn (78) does not involve any structural coupling. Hence, eqn (78) can be written in matrix notation as

$$(c_e-f_{\mathrm{p},e}^{\mathrm{ext}})=0\quad e=1,2,\ldots NEL, \tag{79}$$

where $f_{\mathrm{p},e}^{\mathrm{ext}}$ contains contributions from $W_{\mathrm{p},e}^{\mathrm{ext}}$ as well as from the temporal integration, and the scalar c_e is given by

$$c_e=-A_e\left(\mathbf{B}_{ve}\mathbf{u}_e+\frac{1}{K^{\mathrm{f}}}p_e\right). \tag{80}$$

Finally, the projection problem $\Pi_{\mathrm{p}}(\Omega)$ in eqn (61b) can be written as

$$-\int_{\Omega}\left(f(n)-\frac{\delta}{l_e}\right)[[\tilde{p}']]_e\left(\varepsilon_v+\frac{1}{K^{\mathrm{f}}}p\right)\mathrm{d}\Omega=0. \tag{81}$$

Due to the "orthogonality" conditions (70) and (80), it follows that terms involving continuous portions of ε_v and p will vanish. Hence, eqn (81) may be rewritten as

$$-\int_{\Omega}\left(f(n)-\frac{\delta}{l_e}\right)^2[[\tilde{p}']]_e\left(\frac{1}{\delta}\mathbf{n}\cdot[[\tilde{\mathbf{u}}]]_e+\frac{1}{K^{\mathrm{f}}}[[\tilde{p}]]_e\right)\mathrm{d}\Omega=0. \tag{82}$$

Upon evaluating the integrals in this relationship we may, finally, arrive at the projection problem

$$y_e = -\delta\frac{A_e}{l_e}\left(1-\frac{\delta}{l_e}\right)\left[\frac{1}{\delta}\mathbf{n}^{\mathrm{T}}\cdot[[\tilde{\mathbf{u}}]]_e+\frac{1}{K^{\mathrm{f}}}[[\tilde{p}]]_e\right]=0. \tag{83}$$

5.3. *FE-algorithm*

The pertinent non-linear finite element equations are summarized as

$$\begin{cases} \mathop{\mathbf{A}}_{e=1}^{NEL}\mathbf{g}_e(\mathbf{u}_e,p_e,[[\tilde{\mathbf{u}}]]_e)=\mathbf{0} & \\ c_e(\mathbf{u}_e,p_e)-f^{\mathrm{ext}}_{\mathrm{p},e}=0 & e=1,2,\ldots NEL \\ \mathbf{x}_e(\mathbf{u}_e,[[\tilde{\mathbf{u}}]]_e,[[\tilde{p}]]_e)=\mathbf{0} & e=1,2,\ldots NEL \\ y_e([[\tilde{\mathbf{u}}]]_e,[[\tilde{p}]]_e)=0 & e=1,2,\ldots NEL \end{cases}. \tag{84}$$

A Newton procedure may now be formulated for the coupled problem: From a given iterate (i), compute the improved solution from

$$\begin{cases} \mathbf{u}_e^{(i+1)}=\mathbf{u}_e^{(i)}+\mathrm{d}\mathbf{u}_e \\ p_e^{(i+1)}=p_e^{(i)}+\mathrm{d}p_e \\ [[\tilde{\mathbf{u}}]]_e^{(i+1)}=[[\tilde{\mathbf{u}}]]_e^{(i)}+\mathrm{d}[[\tilde{\mathbf{u}}]]_e \\ [[\tilde{p}]]_e^{(i+1)}=[[\tilde{p}]]_e^{(i)}+\mathrm{d}[[\tilde{p}]]_e \end{cases}, \tag{85}$$

where the increments $\mathrm{d}\mathbf{u}_e$, $\mathrm{d}p_e$, $\mathrm{d}[[\tilde{\mathbf{u}}_e]]$ and $\mathrm{d}[[\tilde{p}_e]]$ are obtained from the proper linearization of eqn (84) at the time $(n+1)$. To this end, we first linearize the solid stress $\boldsymbol{\sigma}$ within Ω_e^{b} and $\Omega_e^{\pm}$, which can be written

$$\begin{cases} \mathrm{d}\boldsymbol{\sigma}_{\mathrm{b}}=\mathbf{E}_{\mathrm{ab}}\mathbf{B}_e\,\mathrm{d}\mathbf{u}_e+\dfrac{1}{\delta}\left(1-\dfrac{\delta}{l_e}\right)\mathbf{E}_{\mathrm{ab}}\mathbf{C}_e\,\mathrm{d}[[\tilde{\mathbf{u}}]]_e \\ \mathrm{d}\boldsymbol{\sigma}_{\mathrm{c}}=\mathbf{E}_{\mathrm{ac}}\mathbf{B}_{\mathrm{e}}\,\mathrm{d}\mathbf{u}_{\mathrm{e}}-\dfrac{1}{l_e}\mathbf{E}_{\mathrm{ac}}\mathbf{C}_e\,\mathrm{d}[[\tilde{\mathbf{u}}]]_e \end{cases}, \tag{86}$$

where $\mathbf{E}_{\mathrm{ab}}$ and $\mathbf{E}_{\mathrm{ac}}$ are algorithmic tangent stiffness matrices pertinent to $\boldsymbol{\sigma}_{\mathrm{b}}$ and $\boldsymbol{\sigma}_{\mathrm{c}}$ respectively. Upon inserting eqn (86) into the linearized version of eqn (84), we obtain the coupled tangent relationship at the elemental level

$$\begin{bmatrix} \mathrm{d}\mathbf{b}_e \\ \mathrm{d}c_e \\ \mathrm{d}\mathbf{x}_e \\ \mathrm{d}y_e \end{bmatrix} = \begin{bmatrix} \mathbf{S}_e & \mathbf{P}_e & \mathbf{F}_e & \mathbf{0} \\ \mathbf{P}_e^{\mathrm{T}} & -M_e & \mathbf{0} & 0 \\ \mathbf{F}_e^{\mathrm{T}} & \mathbf{0} & \mathbf{H}_e & \mathbf{G}_e \\ \mathbf{0} & 0 & \mathbf{G}_e^{\mathrm{T}} & R_e \end{bmatrix} \begin{bmatrix} \mathrm{d}\mathbf{u}_e \\ \mathrm{d}p_e \\ \mathrm{d}[\tilde{\mathbf{u}}]_e \\ \mathrm{d}[\tilde{p}]_e \end{bmatrix}, \tag{87}$$

where

$$\mathbf{S}_e = A_e\left(1-\frac{\delta}{l_e}\right)\mathbf{B}_e^{\mathrm{T}}\mathbf{E}_{\mathrm{ac}}\mathbf{B}_e+A_e\frac{\delta}{l_e}\mathbf{B}_e^{\mathrm{T}}\mathbf{E}_{\mathrm{ab}}\mathbf{B}_e \tag{88a}$$

$$\mathbf{P}_e = A_e\mathbf{B}_{ve}^{\mathrm{T}} \tag{88b}$$

$$\mathbf{F}_e = -\frac{A_e}{l_e}\left(1-\frac{\delta}{l_e}\right)(\mathbf{B}_e^{\mathrm{T}}\mathbf{E}_{\mathrm{ac}}\mathbf{C}_e-\mathbf{B}_e^{\mathrm{T}}\mathbf{E}_{\mathrm{ab}}\mathbf{C}_e) \tag{88c}$$

$$M_e = A_e \frac{1}{K^{\mathrm{f}}} \tag{88d}$$

$$\mathbf{H}_e = \frac{A_e}{l_e}\left(1-\frac{\delta}{l_e}\right)\left[\frac{1}{l_e}\mathbf{Q}_{\mathrm{ac}}+\left(\frac{1}{\delta}-\frac{1}{l_e}\right)\mathbf{Q}_{\mathrm{ab}}\right] \tag{88e}$$

$$\mathbf{G}_e = -\frac{A_e}{l_e}\left(1-\frac{\delta}{l_e}\right)\mathbf{n} \tag{88f}$$

$$R_e = -\delta\frac{A_e}{l_e}\left(1-\frac{\delta}{l_e}\right)\frac{1}{K^{\mathrm{f}}}, \tag{88g}$$

where $\mathbf{Q}_{\mathrm{a}}$ is the algorithmic acoustic matrix that is associated with $\mathbf{E}_{\mathrm{a}}$, i.e. we have $\mathbf{Q}_a = \mathbf{C}_e^{\mathrm{T}}\mathbf{E}_{\mathrm{a}}\mathbf{C}_e$.

It follows that $\mathrm{d}p_e$, $\mathrm{d}[[\tilde{\mathbf{u}}]]_e$ and $\mathrm{d}[[\tilde{p}]]_e$ can be eliminated at the element level, whereby $\mathrm{d}\mathbf{u}_e$ can be obtained from the structural problem

$$\mathop{\mathbf{A}}_{e=1}^{NEL}[\hat{\mathbf{S}}_e^{(i)}\,\mathrm{d}\mathbf{u}_e = -\hat{\mathbf{g}}_e^{(i)}], \tag{89}$$

where the involved (part-inverted) quantities are defined as

$$\hat{\mathbf{S}}_e = \mathbf{S}_e+\mathbf{P}_e M_e^{-1}\mathbf{P}_e^{\mathrm{T}}-\mathbf{F}_e\hat{\mathbf{H}}_e^{-1}\mathbf{F}_e^{\mathrm{T}} \tag{90a}$$

$$\hat{\mathbf{H}}_e = \mathbf{H}_e+\mathbf{G}_e R_e^{-1}\mathbf{G}_e^{\mathrm{T}} \tag{90b}$$

$$\hat{\mathbf{g}}_e^{(i)} = \mathbf{g}_e^{(i)}+\mathbf{C}_e M_e^{-1}(c_e^{(i)}-f_{\mathrm{p},e}^{\mathrm{ext}})-\mathbf{F}_e\hat{\mathbf{H}}_e^{-1}\hat{\mathbf{x}}_e^{(i)} \tag{90c}$$

$$\hat{\mathbf{x}}_e^{(i)} = \mathbf{x}_e^{(i)}+\mathbf{G}_e R_e^{-1}y_e^{(i)}. \tag{90d}$$

When $\mathrm{d}u_e$ has been solved, the internal element quantities can be "post-processed" from the relationships

$$\mathrm{d}[[\tilde{\mathbf{u}}]]_e = -\hat{\mathbf{H}}_e^{-1}(\hat{\mathbf{x}}_e^{(i)}+\mathbf{F}_e^{\mathrm{T}}\,\mathrm{d}\mathbf{u}_e) \tag{91a}$$

$$\mathrm{d}p_e = -M_e^{-1}(-c_e^{(i)}-\mathbf{C}_e^{\mathrm{T}}\,\mathrm{d}\mathbf{u}_e) \tag{91b}$$

$$\mathrm{d}[[\tilde{p}]]_e = -R_e^{-1}(\hat{y}_e^{(i)}+\mathbf{G}_e^{\mathrm{T}}\hat{\mathbf{H}}_e^{\mathrm{T}}\mathbf{F}_e^{\mathrm{T}}\,\mathrm{d}\mathbf{u}_e), \tag{91c}$$

which $\hat{y}_e^{(i)}$ is defined as

$$\hat{y}_e^{(i)} = y_e^{(i)}+\mathbf{G}_e^{\mathrm{T}}\hat{\mathbf{H}}_e^{-1}\hat{\mathbf{x}}_e^{(i)}. \tag{92}$$

6. NUMERICAL EXAMPLE

6.1. *Elastic–plastic model for soil*

The proposed finite element method is used to analyze the behavior of a plane strain specimen subjected to compression, as shown in Fig. 3. To this end, a plasticity model for soil of Mohr–Coulomb type will be used. The main purpose of the model is to describe the nonlinear stress–strain relationship of a frictional material with strongly non-associative volumetric behavior. Similar models have previously been analyzed by, for example, de Borst (1988) and Leroy and Ortiz (1989). The yield criterion F and the flow potential G are defined as

$$F(p,q,\kappa) = q-\eta(\kappa)(p-p_{\mathrm{c}}) \tag{93a}$$

$$G(p,q) = q-\mu(p-p_{\mathrm{c}}), \tag{93b}$$

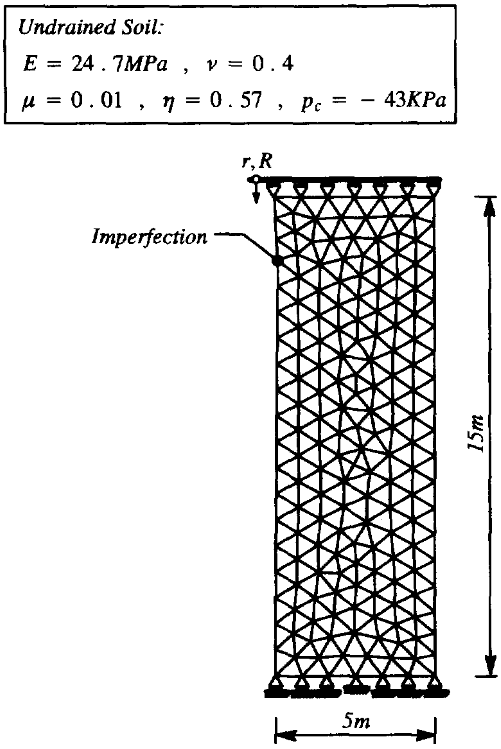

Fig. 3. Geometry, loading and material properties for the compressed plane strain specimen.

where p_c is the cohesion, $\eta = \sin\phi$ (with ϕ = friction angle) and $\mu = \sin\psi$ (with ψ = dilatation angle). Moreover, the invariants p and q in eqn (93a, b) are the (in-plane) solid pressure p and the (in-plane) solid stress deviator q. These are related to the "current" principal values of the solid stress tensor $\boldsymbol{\sigma}$ as

$$q = \tfrac{1}{2}(\sigma_1 - \sigma_3), \quad \sigma_1 \geqslant \sigma_2 \geqslant \sigma_3 \tag{94a}$$

$$p = -\tfrac{1}{2}(\sigma_1 + \sigma_3). \tag{94b}$$

The function $\eta(\kappa)$ in eqn (93a) is proposed as

$$\eta(\kappa) = \begin{cases} \eta(0) + 2\dfrac{\sqrt{\kappa/\kappa_f}}{1+\kappa/\kappa_f}(\bar{\eta} - \eta(0)) & \text{if } \kappa < \kappa_f \\ \eta(\kappa_f) = \bar{\eta} & \text{if } \kappa \geqslant \kappa_f \end{cases}, \tag{95}$$

where $\bar{\eta} = \eta(\kappa_f)$ is the peak value. We also define the evolution rule for the hardening variable κ as

$$\dot{\kappa} = \dot{\lambda}\frac{\partial G(p,q)}{\partial q} = \dot{\lambda}, \tag{96}$$

which means that κ represents the plastic portion of the effective (in-plane) shear strain.

6.2. *Compressed plane strain specimen*

The specimen in Fig. 3 is considered in the numerical evaluation. The loading consists of prescribed horizontally uniform displacement r, which is applied in 100 load steps, at the top of the specimen. An embedded localization band is activated with the critical orientation $\mathbf{n}_{cr}$ at the state when $H \leqslant H_{u,cr}$ has been obtained in some element. This means that the localization bands appear progressively as the loading is increased. In order to

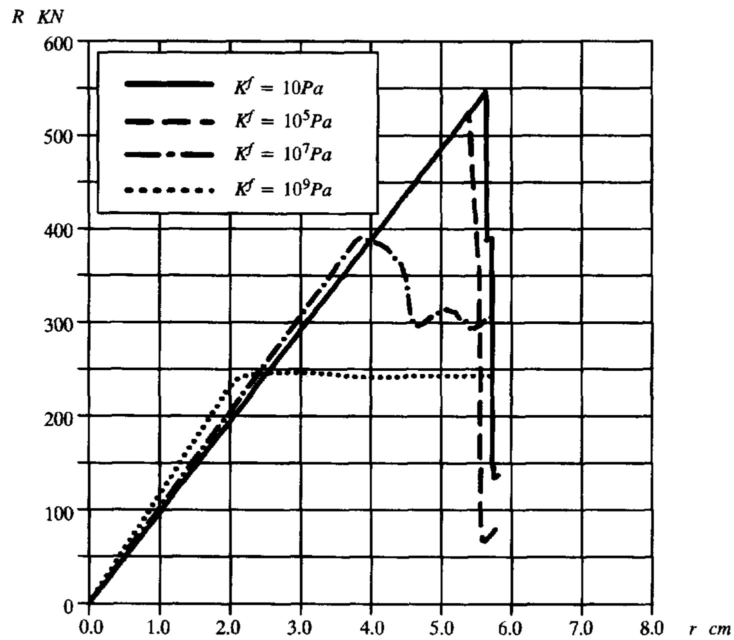

Fig. 4. Load displacement relations for an undrained slope at various choices of pore fluid compressibility ($\delta = 20$ cm).

simplify the numerical implementation, perfectly plastic response is considered in the material model, whereby the condition $H \leqslant H_{u,cr}$ is obtained right at the onset of plastic deformation for some (small) value of K^f. Hence, to obtain localization in the completely incompressible case requires a sufficient amount of softening in the material model (as discussed subsequently). However, in the present analysis, the only cause of pre-peak destabilization is the volumetric non-associativity.

In the investigation, the response is considered when the pore fluid compression modulus K^f ranges from $K^f = 10^1$ Pa, which corresponds essentially to drained response, up to $K^f = 10^9$ Pa, which corresponds to almost incompressible behavior. The results are shown in Fig. 4, where it is observed (as expected) that the pre-peak response becomes "stiffer" as the value of K^f is increased. Moreover, it is noted that the peak load is very sensitive to the value of K^f. For example, in the "drained" situation ($K^f = 10^1$ Pa) the peak load is $R \approx 550$ kN while for $K^f = 10^7$ Pa the peak load is $R \approx 380$ kN. As to the decay of R in the post-peak response, it is noted that a more brittle behavior is obtained as the value of K^f decreases. In fact, for the extreme values of $K^f = 10^1$ Pa and $K^f = 10^9$ Pa almost perfectly brittle and perfectly plastic response is obtained, respectively. The reason is that the value of $\bar{H}_u < 0$, which determines the predicted amount of softening for a given value of δ, tends to zero (and eventually becomes positive) as the value of K^f is increased.

The discussed characteristics are also reflected by the deformation patterns that are shown in Fig. 5. It may be noted that the "drained response" corresponds to a highly localized deformation as shown in Fig. 5(ab). In the intermediate situation, shown in Fig. 5(c), between drained and completely incompressible response, the deformation pattern is slightly more diffuse as compared to the undrained response. In the case that $K^f = 10^9$ Pa no pronounced localization is obtained, which we interpret as the situation where the value of $\bar{H}_u$ has been increased above zero, whereby band-shaped localization is no longer feasible.

7. CONCLUDING REMARKS

On the basis of the developments in Larsson and Runesson (1995), we have extended the concept of a regularized displacement discontinuity for the one-phase material to a mixture of a solid phase and a pore fluid phase subjected to undrained conditions. The key issue in the developments is the generalization of the momentum and mass balance, for the one phase material, into the corresponding relationships for the mixture.

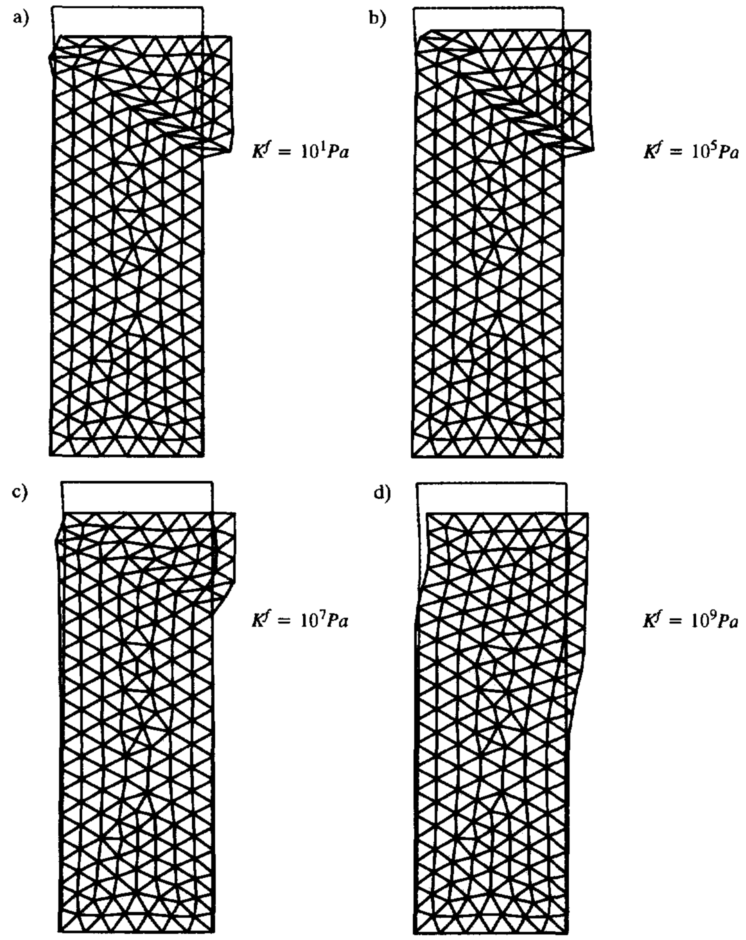

Fig. 5. (a–d) Deformation patterns at final load step for various choices of K^f.

As a result a generalized criterion of band-shaped localization was obtained, which couples the matching displacement and pore pressure discontinuities. The consequence of this criterion was studied with respect to different loading situations inside and immediately outside the localization band. In particular, it appears that band shaped localization is not possible until the actual hardening modulus becomes smaller than the critical value, which represents the singularity of the *undrained* acoustic tensor.

As to the boundary value problem, a mixed variational formulation was proposed to capture regularized discontinuities in the spirit of the enhanced strain formulation of Simo and Rifai (1990). A simple finite element, based on the CST-element, was proposed in such a fashion that the pore pressure and the discontinuities (in displacement and pore pressure) can be resolved at the element level. In this way it is possible to obtain a displacement formulation at the structural level. The proposed element was successfully implemented together with a simple frictional material model for soil, and the results indicate the strong influence of the pore fluid compressibility on the structural behavior.

REFERENCES

de Borst, R. (1988). Bifurcation in finite element with a non-associated flow law. *Int. J. Numer. Anal. Meth. Geomech.* **12,** 99–116.

Desrue, J., Chambon, R., Mokni, M. and Mazerolle, F. (1993). Void ratio evolution inside shear bands in triaxial sand samples studied by Tomodensiometry. (Abstract) *Proc. of 3rd Workshop on Localization and Bifurcation Theory for Soils and Rocks*, Aussois 6–9 September 1993, France.

Larsson, R., Runesson, K. and Ottosen, N. S. (1993). Discontinuous displacement approximation for capturing plastic localization. *Int. J. Numer. Meth. Engng* **36,** 2087–2105.

Larsson, R. and Runesson, K. (1996). Element-embedded localization band based on regularized strong discontinuity. *J. Engng Mech. ASCE* (in press).

Leroy, Y. and Ortiz, M. (1989). Finite element analysis of strain localization in frictional materials. *Int. J. Numer. Anal. Meth. Geomech.* **13,** 53–74.

Loret, B. and Prevost, J. H. (1990). Dynamic strain localization in fluid-saturated porous media. *Second World Congress on Computational Mechanics*, International Association of Computational Mechanics, Stuttgart, FRG, 27–31 August, 278–281.

Ottosen, N. S. and Runesson, K. (1991). Properties of bifurcation solutions in elasto-plasticity. *Int. J. Solids Struct.* **27,** 401–421.

Rudnicki, J. W. (1983). A formulation for studying coupled deformation and pore fluid diffusion effects on localization of deformation. *Proc. of the Symp. on the Mechanics of Rocks, Soils and Ice, ASME* (Edited by S. Nemat-Nasser), p. 35–44. ASME, New York.

Runesson, K., Peric, D. and Sture, S. (1996). Effect of pore-fluid compressibility on localization in elastic–plastic porous solids. *Int. J. Solids Structures* (in press).

Simo, J. C. and Rifai, M. S. (1990). A class of mixed assumed strain methods and the method of incompatible modes. *Int. J. Numer. Meth. Engng* **29,** 1595–1638.

Simo, J. C., Oliver, J. and Armero, F. (1993). An analysis of strong discontinuities induced by strain-softening in rate-independent solids. *Comput. Mech.* **12,** 277–296.